

## A PICTURE BOOK OF TWO FAMILIES OF CUBIC MAPS

FERNANDO CABRAL,<sup>a,b</sup> ALEXANDRE LAGO<sup>a</sup> and JASON A. C. GALLAS<sup>a,c,d</sup>

<sup>a</sup>*Laboratório de Óptica Quântica da UFSC  
88040-900 Florianópolis, SC, Brazil*

<sup>b</sup>*School of Mathematics and Statistics  
The University of Birmingham, Birmingham, B15 2TT, UK*

<sup>c</sup>*Laboratory for Plasma Research, University of Maryland  
College Park, MD 20742-3511, USA*

<sup>d</sup>*HLRZ Supercomputing Center, KFA  
D-5170 Jülich, Germany*

Received 5 November 1992

This paper reports high-resolution isoperiodic diagrams for two model-families of dynamical systems characterised by one-dimensional maps depending on two parameters. We present a comparison of both diagrams, investigating the way in which initial conditions affect isoperiodic sets in the parameter space of both systems and the similarities between them. Although both models represent quite different dynamical systems, they are found to have many properties in common in their space of parameters.

*Keywords:* Isoperiodic Diagrams; Cubic Maps; Chaotic Dynamical Systems.

### 1. Introduction

The present paper reports high-resolution isoperiodic diagrams on the parameter space of two families of dynamical systems modeled by cubic polynomials and presents a comparison between them. The two models considered are defined by the maps

$$x_{t+1} = -x_t(x_t^2 - a) - b, \quad (1)$$

and

$$x_{t+1} = +x_t(x_t^2 - a) - b. \quad (2)$$

While it is easy to reduce general cubic mappings to one of the above forms, there is no change of variable able to transform Eq. (1) into Eq. (2) and vice versa. Therefore, these two dynamical systems are independent of each other. In fact, the two forms above seem to be the basic normal forms for 1D cubic maps.

During this century, cubic maps were major participants in two moments when significant advances in our understanding of dynamical systems were done. They were important for Fatou<sup>1</sup> and Julia<sup>2</sup> while laying down the foundations for the modern study of dynamics by analysing among other things, polynomials in the

complex plane. Cubic maps were again ‘central figures’ about 50 years later, during pioneering work with computers in dynamics. Many topics which are present-day subjects of very active research appear clearly in a fundamental contribution by Stein and Ulam<sup>3</sup> entitled “Non-linear transformation studies on electronic computers”, where these authors not only investigate the dynamics of transformations in general but present a clear view and preview of their impact in general. This important contribution, written in English, has not been recognized so far as widely as it perhaps deserved. The paper by Stein and Ulam was reprinted in the book, *Stanislaw Ulam: Sets, Numbers and Universes*,<sup>4</sup> collecting a number of papers by Ulam. The book appeared in 1974, i.e., *slightly ahead* of the official birth and impact of ‘chaology’. At the end of the book the various contributions of Ulam are commented by several authors. It is interesting to read today what Stein wrote on page 697 of the book, about his *Polish paper* with Ulam:

“This paper is open to the criticism that it fails to indicate promising lines for the theoretical study of the nonlinear phenomena which Ulam and Stein discuss. As shown by the references quoted above, the appropriate tools for such study are in the process of development, but one is a long way from being able to cope with the apparently pathological behavior exhibited by even the simple class of transformations treated in this paper. At the present writing, therefore, it seems clear that the development of adequate theoretical methods will have to be preceded by further numerical experimentation, some of which will differ only in precision and level of sophistication from that exemplified by this paper and that of Metropolis, Stein, and Stein.”

Equations (1) and (2) are invariant to the simultaneous transformation of  $x \rightarrow -x$  and  $b \rightarrow -b$ . For  $b = 0$ ,  $x_0 = 0$  is a fixed point. As is known, the sign difference between these systems implies changes in several dynamical aspects of the models. To uncover what common regularities these systems might have in the space of parameters and how generic are such regularities as both parameters vary, we recorded periodicities found by iterating the above equations from a given common initial value  $x_0$ . The idea is to investigate for both models the way in which sets of parameters  $(a, b)$  characterized by isoperiodic orbits organize themselves and to contrast them. The present paper is intended to present a qualitative view of the rich topology observed in the parameter space of the dynamical systems represented by the normal forms in Eqs. (1) and (2) above. A comprehensive quantitative analysis will be presented elsewhere. A previous paper<sup>5</sup> introduced ‘isoperiodic diagrams’ as a convenient tool to investigate the parameter space of dynamical systems and presented a heuristic analysis of the topology of the parameter space for the Hénon map. In many ways, these three dynamical systems share a lot of common features. Since such features are robust and apparently independent of the map involved,

they are conjectured to be generic for other dynamical systems too. Of course, the precise delimitation of such ‘genericity’ remains to be investigated.

Before finishing this introduction there is an important point to note. After submitting this ‘picture-book’ for publication we were able to obtain a full copy of a book by Mira.<sup>6</sup> This book presents many references related with the dynamics of one- and two-dimensional maps, several of them which we could not yet access or study properly. The book contains a description of how to get shrimps using the concept of ‘multipliers’ which, as explained by Mira, was so useful to Fatou and to Julia during the first 20 years of this century, to Myrberg (1957–63), to Mira (1967–87) and coworkers and many others. It also presents figures with accurate contours of the innermost domains of the first few shrimps for the Hénon map and many others figures that help to understand what is contained in the figures of Ref. 5 and here. It is instructive to present here a brief description of how one can ‘easily’ obtain the boundaries of shrimps. For an extended discussion we refer the reader to Mira,<sup>6</sup> which also gives many early references. In a future publication we will review this subject to include the many important recent developments (done during the last decade or so and not found in Ref. 6) under a much needed *historical* perspective, after considering the voluminous literature cited in Ref. 6 which lack of time prevented us from studying so far. For the moment let it be said that there is in the literature of the last 10 years or so a number of important works discussing the parameter space of dynamical systems, most notably of the circle and related maps. But from what Mira writes it also appears that there is a ‘discontinuity’ in the literature somewhere, an issue that is premature for us to address at present.

For a dynamical system defined by a generic recurrence relation  $x_{t+1} = f(x_t, p)$ ,  $p$  representing one or several parameters, one studies the stability of the fixed points  $x_c$ , which obey  $x_c = f(x_c, p)$ . For these points one then considers the *multiplier*

$$m = f'(x_c, p),$$

and its modulus  $M = |m|$ . A fixed point  $x_c$  is *attracting* if  $M < 1$ , is *repelling* if  $M > 1$  and *indifferent* if  $M = 1$ . *Superstable* points are those for which  $M = 0$ . The *boundaries* in the parameter space of the domain containing attracting fixed points are then obtained by ‘sweeping’ the parameter(s)  $p$  and recording the values of those  $p$  for which  $m = +1$  or  $m = -1$ . This procedure generates the innermost boundary of the ‘period-1 shrimp’  $1 \times 2^n$ . To obtain the boundaries of any period  $k$  one needs to replace  $f(x, p)$  by its higher ‘compositions’  $f^{(k)}(x, p)$  and observe that the complicate derivative  $f^{(k)'}(x, p)$  that will then appear in the definition of  $m$  can be easily reduced to the multiplication of several  $f'(x_i, p)$  evaluated at the periodic cycle  $x_i$ ,  $i = 1, 2, \dots, k$ . From this one understands why  $m$  was called **multipliqueur**. Undoubtedly, it is a neat useful tool. It surely explains the whole internal structure of the shrimps. The challenge seems now to be to understand *how* and *why* they all appear aligned.

## 2. Computational Details

All isoperiodic diagrams discussed below were obtained by considering a fine rectangular mesh over certain  $a \times b$  domains of the parameter space. The range of  $a$  was divided into 1142 equally spaced segments (horizontal resolution) and that of  $b$  into 826 segments (vertical resolution). As previously done for the Hénon map,<sup>5</sup> each  $(a, b)$  ‘pixel’ was then colored according to the characteristic periodicity found by restarting calculations always from a given initial point  $x_0$ , after a convenient number of preiterates, 1000 most of the times. Reducing this value to 200 produced differences that could only hardly be seen in the pictures, appearing mostly at the boundaries between isoperiodic domains. Upon iteration, orbits either converge to unbounded attractors or remain confined to very particular sets having periodicities 1, 2, 3, . . . . Similarly to familiar bifurcation diagrams, there is a “practical limit” in the actual computation of the periodicities as well as a “visual limit” regarding the amount of different periods that can be properly represented on a given graph within a specified domain and resolution. These limits can be conveniently extended by zooming into specific domains of the  $a \times b$  space. In this way it is possible to paint the parameter space with different colors, according to the periodicity of the final attractor to which the system evolved. Such ‘cartographic’ parameter-plane representation depends on the initial condition used to start the iteration at every  $(a, b)$  point. Such dependence is important and is considered with details below.

The computations reported here were performed on a network of three SUN Sparc-2 stations running in parallel and using double precision arithmetic (16 digits). A few test-runs using extended double precision (32-digits), done using also a CONVEX C-210 computer, showed no noticeable differences. Increasing the transient time to 2000 preiterates had practically no effect on the pictures. Therefore we believe all phenomena reported to be stable non-transient intrinsic behaviors of the cubic maps. Bounded orbits were considered as having period  $k$  if after preiteration they displayed a sequential repetition of patterns given by  $x_i = x_{i+k} = x_{i+2k}$ . Otherwise they were considered “chaotic”. In actual computations we considered periods  $k$  up to 64. Rather than an intrinsic limitation of the computer program, this value is mainly dictated by the *visual resolution limit* reached quickly by the fast rate with which isoperiodic regions of high periods diminish. A finite palette of colors as the one defined in Fig. 1a can be conveniently ‘recycled’ to display the way in which the several sets having common periods are internally organized according to a  $k \times 2^n$  route. In the present pictures, chaotic behavior was indicated in white while periods 1, 2, . . . were painted using colors as defined in the table of Fig. 1a. On a few occasions we have changed the colors used to represent parameters corresponding to unbounded attractors. Such changes are clearly indicated below.

### 3. The map $x_{t+1} = -x_t(x_t^2 - a) - b$

In addition to the color table, Fig. 1 shows the isoperiodic region contained in the rectangle delimited by  $-2.0 \leq a \leq 4.0$  and  $-3.0 \leq b \leq 3.0$ . This figure provides a

broad overview of the space of parameters and shows distortions and asymmetries induced when starting iterations from different initial conditions  $x_0$ . In this figure we use black to represent  $(a, b)$  pairs for which trajectories go to the attractor at  $+\infty$ , purple for trajectories going to  $-\infty$  while white is used to color all pixels for which the trajectory is chaotic. From Fig. 1 it is possible to see the very regular way in which the several  $(a, b)$  sets characterized by motions having the same periodicity are organized. Both ‘basins of infinity’ are peculiarly intertwined. The extent of each domain corresponding to attractors at infinity slightly depends on the actual numerical value taken as the “numerical infinity” in the calculations, i.e., the point at which our algorithm concludes trajectories to be diverging. The intertwined structure can be regarded as indicating the ‘gradient’ with which trajectories diverge. The black and purple colors shown in the figures reflect the *sign* of  $x_i$  at the precise moment that the algorithm concluded the trajectory to be diverging. The blue oval located at about the center of Fig. 1b corresponds to fixed points having  $k = 1$ . There are two *chaotic seas* located roughly parallel to the main and secondary diagonals of the pictures. The somewhat loose ‘parallelism’ to the diagonals is easier to recognize in Fig. 1b. In subsequent figures we will be concentrating on several features found in the *upper chaotic sea*, i.e., along the chaotic sea that is roughly parallel to the main diagonal. For  $x_0 = 0.0$ , this sea is exactly symmetric to that located along the secondary diagonal. By starting from  $x_0 = -0.5$  and  $-1.5$  one simply interchanges the regions where the ‘distortions’ appear.

As is clear from Fig. 1, the structures present in the parameter space are strongly distorted as initial conditions change but with islands inside the chaotic sea remaining essentially independent of  $x_0$ . There is a symmetric reciprocity of distortions due to interchanges of  $x_0$  by  $-x_0$  (not shown in the figures). It is also possible to recognize very wide ranges of parameters for which finite attractors exist. Figure 1 clearly shows extended regions where more than one attractor is present. Such regions present rich hysteretic behaviors sensitively dependent on initial conditions and on the particular path followed while moving in the space of parameters. From Fig. 1 it is easy to see the rather complicated entangling of the parameter space. The multicolor fish-like structure in the middle of Fig. 1b is the *union* of all parameters for which the dynamics is either periodic or chaotic. We now concentrate on this fish-like structure and describe several phenomena observed in it.

The most prominent feature in Fig. 1b is the large blue region corresponding to a fixed point (period-1 orbits). When moving from left to right one finds adjacent period-2 green domains, which further ‘bifurcate’ into a period-4 red domain and so on. Although there is a clear period-doubling route to chaos (chaos is painted white), subsequent regions corresponding to higher periods are increasingly difficult to see in the scale of this figure. A salient feature in the figures is the reflection symmetry with respect to the  $b = 0$  line. Embedded in the chaotic seas one finds complex shrimp-like structures. Such shrimps are similar to those found for the Hénon map.<sup>5</sup>

Figure 2 is an enlargement of the upper domain where chaotic behavior is predominant. It clearly shows that the space of parameters contains an enormously large number of self-similar shrimp-shaped structures. Such structures are encountered at all possible scales of magnification and having all possible periods. There are several different shrimps having the same period. One particularly interesting feature that can be clearly recognized is the possibility of going by properly adjusting  $a$  and  $b$ , from almost any periodic domain *directly* into either a chaotic attractor or to the attractors at  $\pm\infty$ . This is particularly easy to see proceeding along one of the ‘scissors legs’ at the end of the biggest shrimp (of period-3, i.e., the light blue structure). Figure 3 shows the recurrence of shrimps along the main chaotic sea. Note that the legs extend along all the white chaotic region, becoming more and more ‘parallel’ as one moves away from the main central bodies. Note also the complicated but very symmetrical way with which shrimps appear at the different levels of magnification indicating self-similarity. It is also important to note that all isoperiodic structures embedded in the chaotic sea appear always with the full cascade  $k \times 2^n$ ,  $k = 1, 2, 3, \dots$ , attached to them.

#### 4. The map $x_{t+1} = x_t(x_t^2 - a) - b$

Isoperiodic diagrams for the map  $x_{t+1} = x_t(x_t^2 - a) - b$  are presented in Figs. 4 to 7. As for the previously considered dynamical system, this one also shows sensitive dependence on initial conditions and hysteresis. Comparing Figs. 1 and 4 one sees that the negative cubic term present in the map bends the white chaotic domains symmetrically toward regions of higher  $a$  values. But the intersection of both upper and lower chaotic regions remains relatively unperturbed along the  $b = 0$  axis. A markedly different behavior is the way in which the two chaotic branches intersect each other in neighborhoods close to the line  $b = 0$ . This is shown in the magnified views presented in Figs. 4c ( $x_0 = 0$ ) and 4d ( $x_0 = 0.5$ ). By comparing both figures it is possible to recognize that one *may* or *may not* navigate along isoperiodic regions and that this possibility depends very much on initial conditions. In the particular case of Fig. 4c, if one insists in sticking to orbits starting at  $x_0 = 0$  while trying to navigate from one period-2 region to the other, it will be necessary to cross a ‘tempestuous chaotic sea’ along the way. In contrast, using orbits from  $x_0 = 0.5$ , at least in one direction it is possible to move without ever noticing any sign of the chaotic sea. This observation is very important for practical applications and shows that in order to assure ‘calm navigation’ (assuming that this is what one wants!) it is not enough to adiabatically change the dynamical parameters of the model: there are still very subtle sensitivities buried in the precise way with which initial conditions vary.

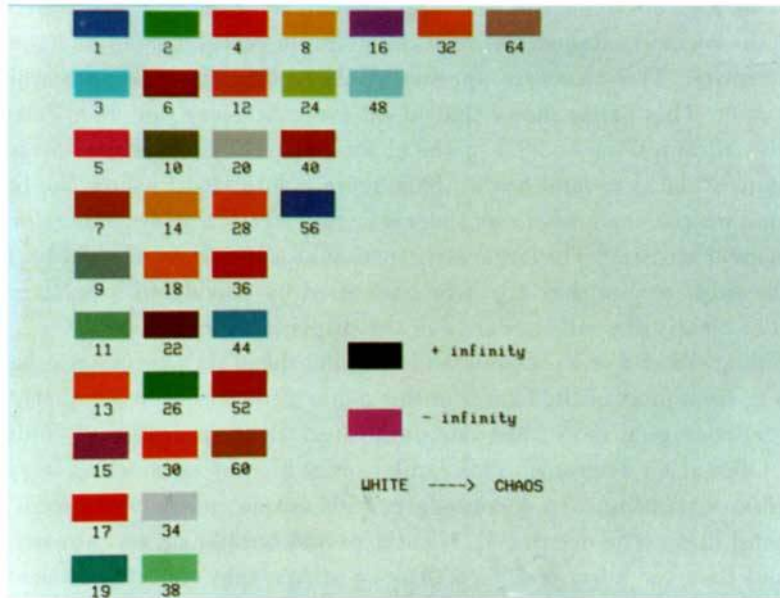
Figure 5 presents details of the typical alignment of shrimps found in two different directions, roughly along and the main chaotic region (Fig. 5a) and roughly perpendicular to it (Fig. 5b). Figure 6a shows under further magnification a region

contained in Fig. 5b along the ‘secondary diagonal’ while Fig. 6b presents more details of the region contained between the period-6 yellow shrimp and the period-8 brown shrimp. This structure appears at the ‘intersection’ of both white arms around  $b = 0$ . This figure shows that at all magnifications one finds “structures-parallel-to-structures” embedded in the chaotic sea. Figure 7 shows a night-view (chaos painted black) around  $b = 0$ . This figure is intended to show the birth of a larger island which occurs whenever there is an ‘intersection’ of two lines along which shrimps appear aligned.<sup>5</sup> The larger structures that ‘survive’ on a bright background and all the substructure that might be uncovered by playing with palettes. These figures show clearly the self-similarity in the displayed domain.

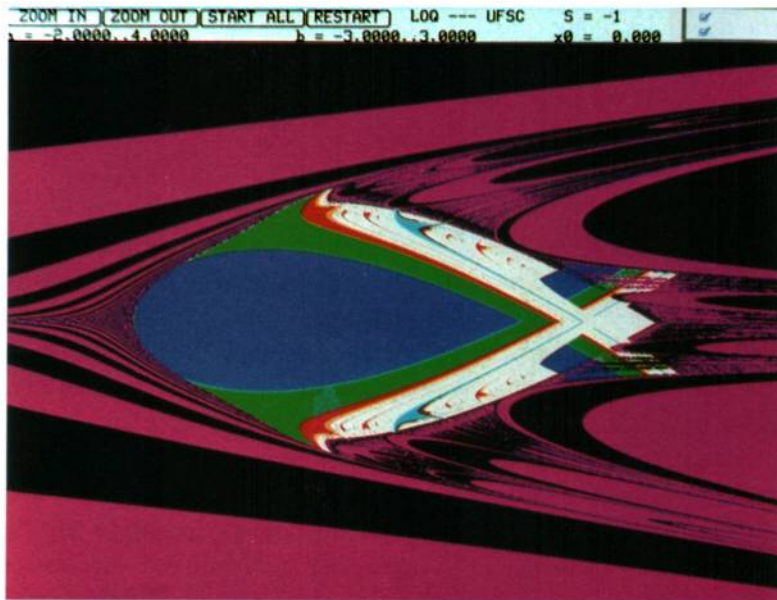
By holding either  $a$  or  $b$  constant while varying the other parameter it is possible to recognize from most of the figures in this paper a phenomenon peculiarly present in maps depending on more than one parameter: the appearance of “bubbles” in standard bifurcation diagrams. This can be easily seen by considering sequences of different first increasing then decreasing periods as one crosses along most vertical or horizontal lines. The occurrence of such ‘period bubblings’ was already noticed by Bier and Bountis<sup>7</sup> a few years ago. Among others, they considered the same two families of dynamical systems discussed here. While they properly report period-bubbling to occur for the map  $x_{t+1} = x_t(x_t^2 - a) - b$ , they incorrectly state that period-bubbling cannot be observed in the map  $x_{t+1} = -x_t(x_t^2 - a) - b$ . By considering the dynamics along constant- $a$  or constant- $b$  lines in the figures presented here one sees that ‘period bubbling’ is in fact present for this normal form of the cubic map as it is for the other one.

## 5. Conclusions

The present paper reports high-resolution isoperiodic diagrams for two families of one-dimensional maps depending on two parameters. Although the maps represent two different dynamical systems, our results show their space of parameters to be very regular and to have similar topology. As also found for the Hénon and some other maps, such space contains many autosimilar shrimp-like isoperiodic islands of the form  $k \times 2^n$  for  $k = 1, 2, 3, \dots$ . From the figures presented here it is easy to recognize that the borders between different isoperiodic islands involve some simple curves, apparently reflecting the equation ruling the eigenvalues of the maps involved. It would be interesting to obtain analytical expressions for the stable borders in isoperiodic diagrams and to discover what kind of ‘renormalization group’ is at work for them, if any. Such work is in progress and will be reported in due course. Another application of the isoperiodic diagrams proposed in Ref. 5 can be found in the investigation of “memory effects” based on *discrete* dynamical system<sup>8</sup> and on the study of piecewise-continuous maps<sup>9</sup> for which, based on previous work by Misiurewicz and others, one might hope to find solid proofs.



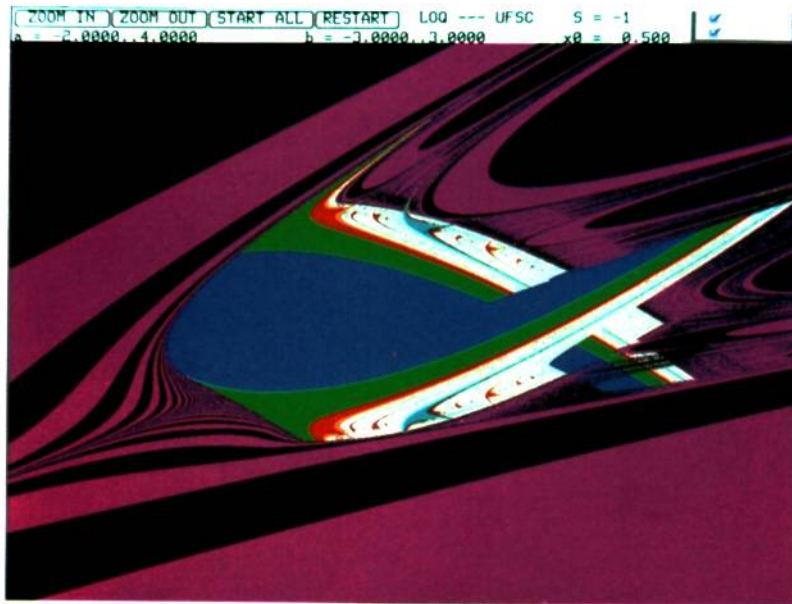
(a)



(b)

Fig. 1. Effect of initial conditions on the bifurcation plane of the cubic  $x_{t+1} = -x_t(x_t^2 - a) - b$ . The basic domain displayed is  $-2.0 \leq a \leq 4.0$  and  $-3.0 \leq b \leq 3.0$ . (a) Table of colors characterizing period-doublings starting at  $k = 1, 3, 5, \dots$ ; (b)  $x_0 = 0.0$ ; (c)  $x_0 = +0.5$ ; (d)  $x_0 = 1.5$ .



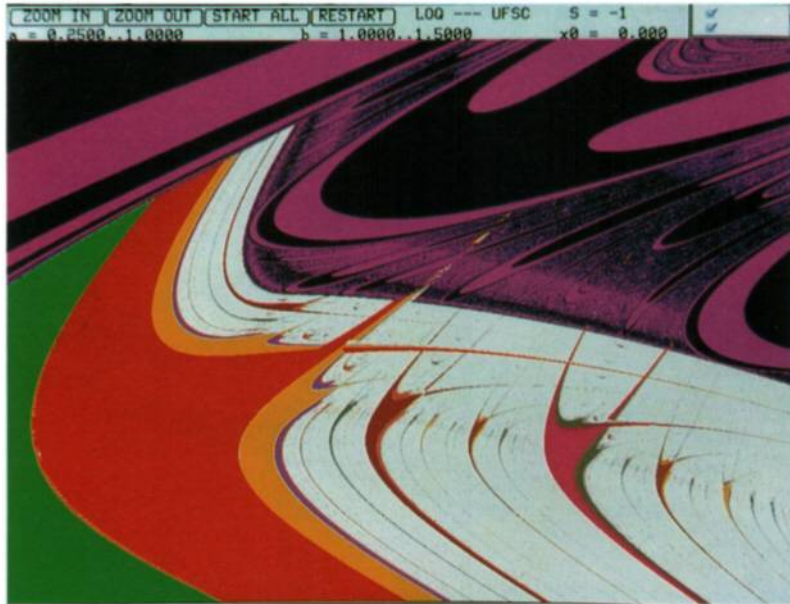


(c)

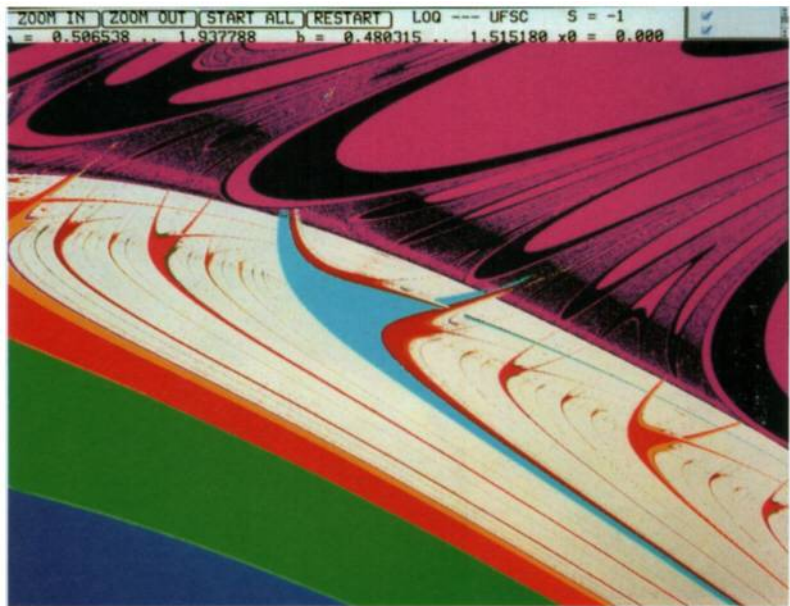


(d)

Fig. 1. (Continued)

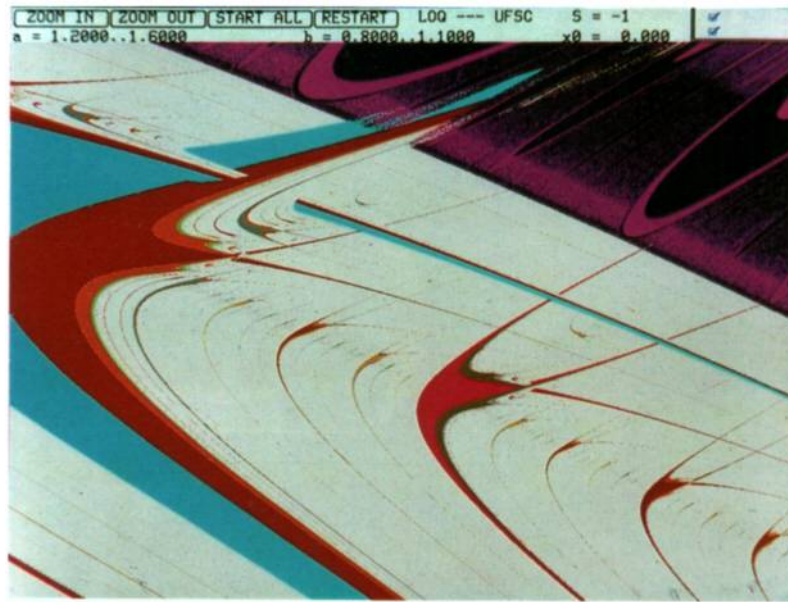


(a)

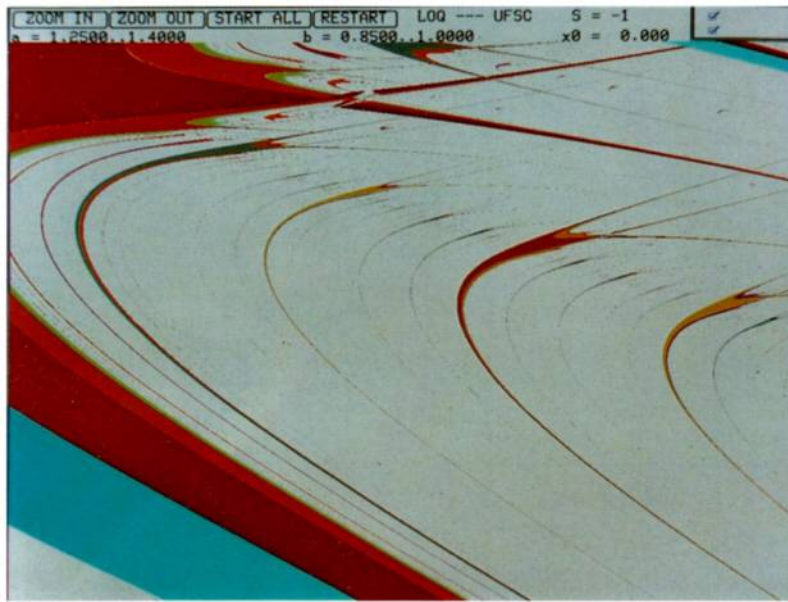


(b)

Fig. 2. Closer views of the periodic structures imbedded in the upper chaotic sea, parallel to the main diagonal of Fig. 1b. Both figures obtained for  $x_0 = 0.0$ . (a) The region  $0.25 \leq a \leq 1.00$  and  $1.00 \leq b \leq 1.50$ . (b) Larger view of the chaotic sea:  $0.506 \leq a \leq 1.937$  and  $0.48 \leq b \leq 1.51$ .

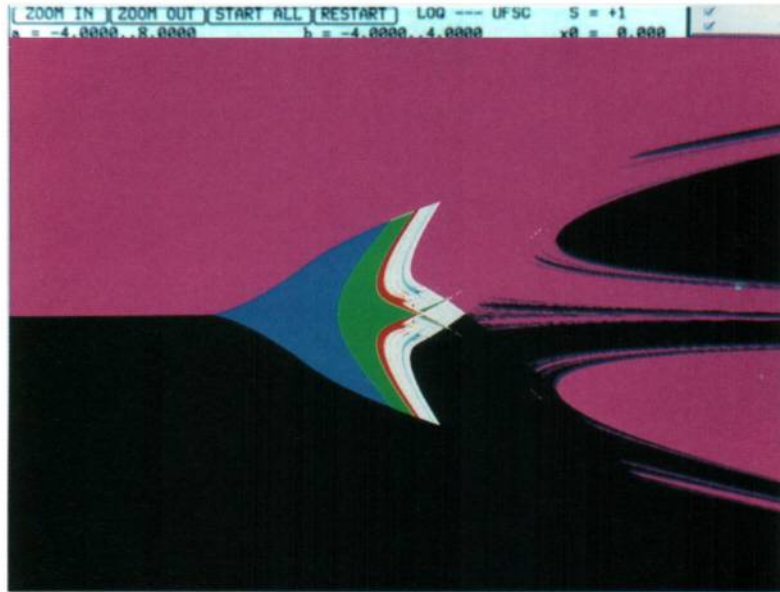


(a)

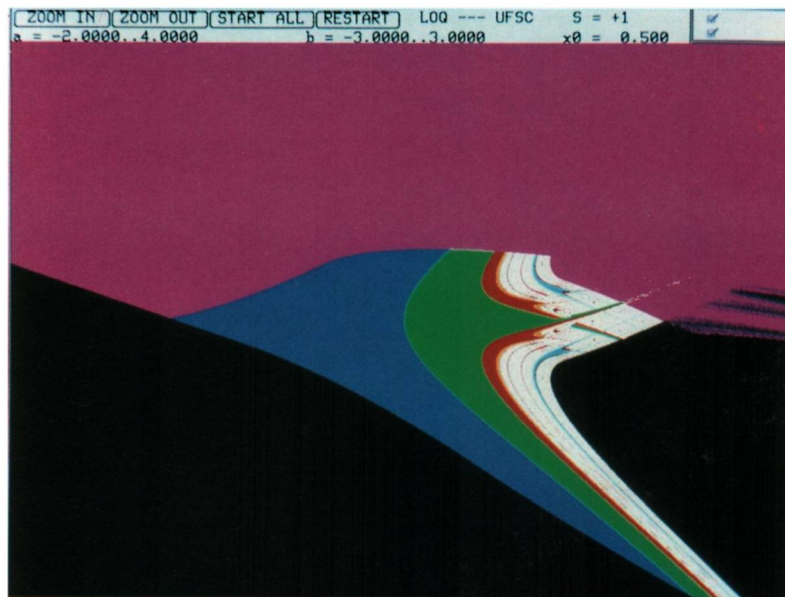


(b)

Fig. 3. Recurrence of the periodic 'shrimps' along the main chaotic sea.  $x_0 = 0.0$ . (a) Zoom of the big light-blue period-3 region of Fig. 2b. Here:  $1.2 \leq a \leq 1.6$  and  $0.8 \leq b \leq 1.1$ ; (b) Zoom of the region between the period-3 and period-5 islands:  $1.25 \leq a \leq 1.40$  and  $0.85 \leq b \leq 1.00$ .

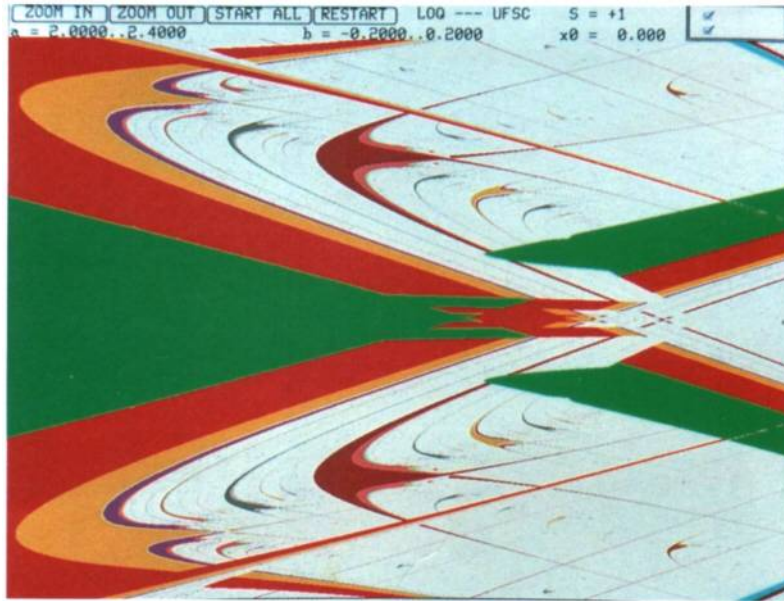


(a)

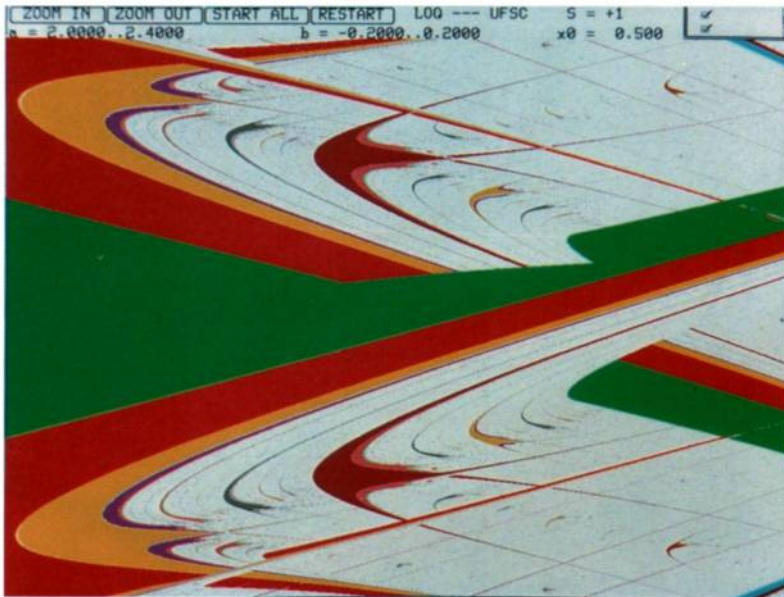


(b)

Fig. 4. Effect of the initial conditions on the map  $x_{t+1} = x_t(x_t^2 - a) - b$ . (a) Larger view:  $-4.0 \leq a \leq 8.0$  and  $-4.0 \leq b \leq 4.0$  for  $x_0 = 0.0$ ; (b) The region  $-2.0 \leq a \leq 4.0$  and  $-3.0 \leq b \leq 3.0$  for  $x_0 = +0.5$ ; (c) The region of “symmetric crossing”:  $2.0 \leq a \leq 2.4$  and  $-0.2 \leq b \leq 0.2$ , for  $x_0 = 0.0$ ; (d) Same region as in (c) but now for  $x_0 = 0.5$ .

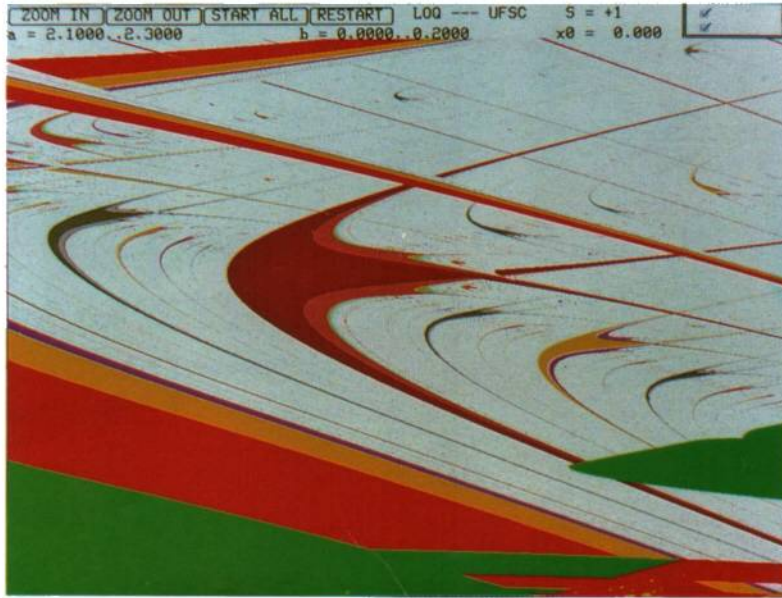


(c)

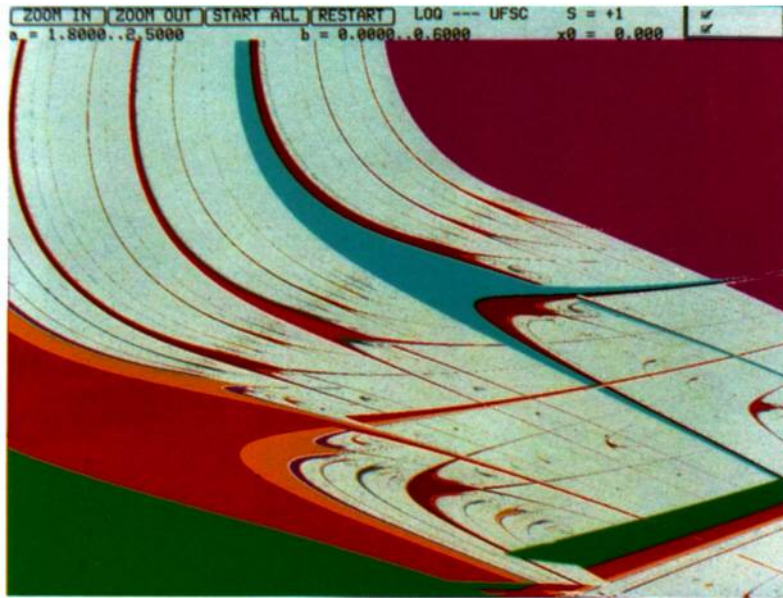


(d)

Fig. 4. (Continued)

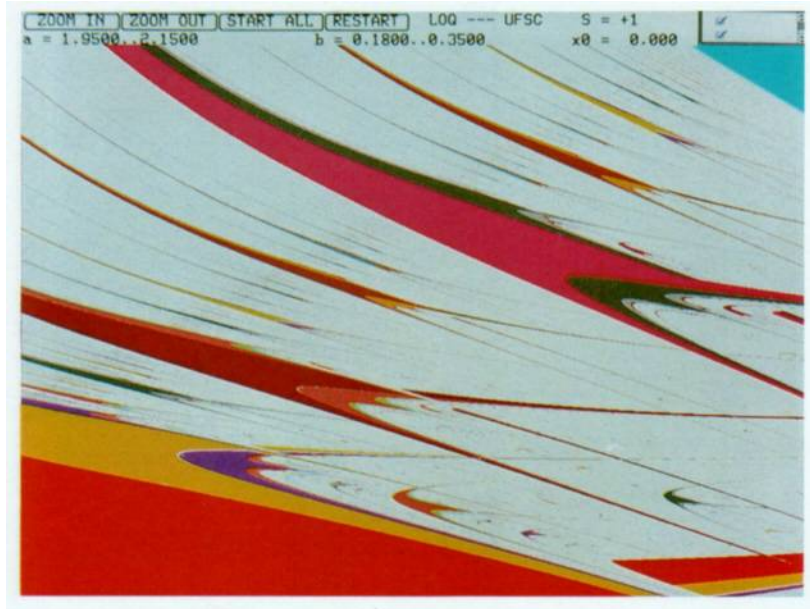


(a)

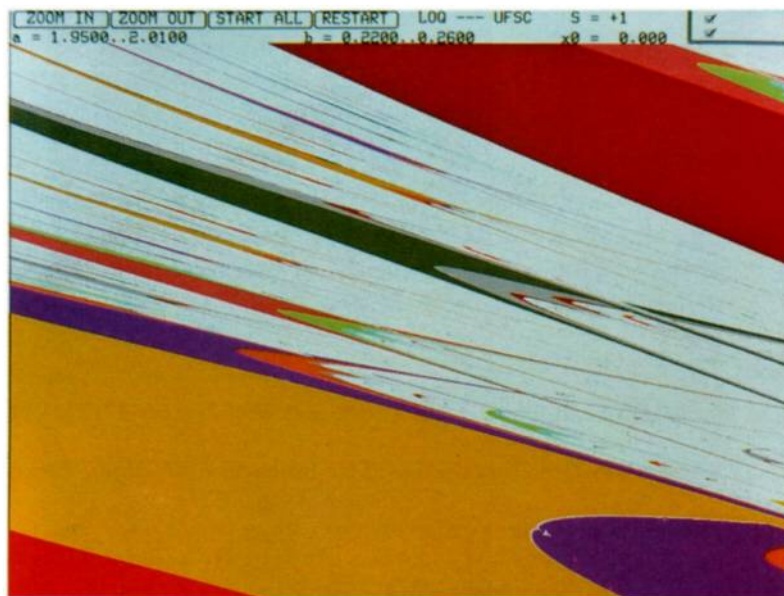


(b)

**Fig. 5.** Details showing for  $x_0 = 0.0$  recurrent structures along the (a) 'main' diagonal in the region  $2.10 \leq a \leq 2.30$  and  $0.0 \leq b \leq 0.2$ ; (b) 'secondary' diagonal:  $1.80 \leq a \leq 2.50$  and  $0.0 \leq b \leq 0.6$ .



(a)



(b)

Fig. 6. Zoom of the 'secondary' diagonal displayed in Fig. 5b. (a)  $1.95 \leq a \leq 2.15$  and  $0.18 \leq b \leq 0.35$ ; (b)  $1.95 \leq a \leq 2.01$  and  $0.22 \leq b \leq 0.26$ . Yellow corresponds to a period-8 shrimp while brown corresponds to period-6.

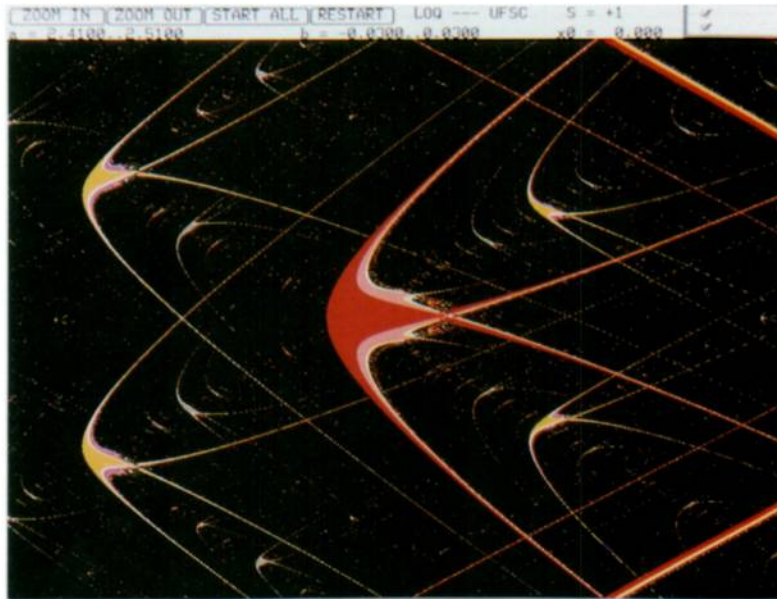


Fig. 7. Night view of the domain  $2.41 \leq a \leq 2.51$  and  $-0.03 \leq b \leq 0.03$ ,  $x_0 = 0.0$ : chaos is represented by black pixels. The larger island in the center corresponds to a period-6 shrimp while the four symmetrically placed shrimps around it have period 8. The larger island results from a 'collision' of the two lines along which shrimps appear aligned and which form the cross roughly along the two diagonals of the figure.

### Acknowledgments

JACG is a Senior Research Fellow of the Conselho Nacional de Pesquisas, CNPq, Brazil, spending a sabbatical year at College Park. He thanks Profs. C. Grebogi and J. A. Yorke for the hospitality, many stimulating discussions and encouragement, and for the privilege of participating in the 'Dynamics Pizza Lunch Seminar'.

### References

1. P. Fatou, "Sur les équations fonctionelles", *Bull. Soc. Math. France* **47**, 161 (1919); *ibid.* **48**, 33 (1920).
2. G. Julia, "Mémoire sur l'iteration des fonctions rationnelles", *J. Math. Pures Appl.* **8**, 47 (1918).
3. P. R. Stein and S. Ulam, *Rozprawy Matematyczne* **39**, 1 (1964).
4. *Stanislaw Ulam: Sets, Numbers and Universes*, edited by W. A. Beyer, J. Mycielski and G. C. Rota (MIT Press, Cambridge, 1974).
5. J. A. C. Gallas, *Int. J. Modern Phys.* **C3**, 1295 (1992).
6. C. Mira, *Chaotic Dynamics — From the One-dimensional Endomorphism to the Two-dimensional Diffeomorphism* (World Scientific, 1987).
7. M. Bier and T. Bountis, *Phys. Lett. A* **104**, 239(1984).
8. J. A. C. Gallas, "Simulating memory effects with discrete dynamical systems", *Physica A*, 1993, in press.
9. J. A. C. Gallas, 1993, work in progress.